

The Influence of the Decay of OB Associations on the Evolution of Dwarf Galaxies

E. P. Kurbatov

Institute of astronomy, Russian Academy of Sciences

48 Pyatnitskaya st., Moscow, Russian Federation, 119017

kurbatov@inasan.ru

Abstract

It is commonly believed that most of the stars born in associations decaying with characteristic velocities of stars ~ 10 km/s. For dwarf galaxies the decay can lead to ejection of stars from the galaxy. The effect is studied for spheroidal and disk dwarf galaxies, and is shown to have substantial observational consequences for disk galaxies with escape velocities up to 20 km/s, or dynamical masses up to $10^8 M_\odot$. The ejection of stars can (i) reduce the abundances of the products of Type Ia supernovae and, to a lesser degree, Type II supernovae, in disk stars, (ii) chemically enrich the galactic halo and intergalactic medium, (iii) lead to the loss of 50% of the stellar mass in galaxies with masses $\sim 10^7 M_\odot$ and the loss of all stars in systems with masses $10^5 M_\odot$, (iv) increase the mass-to-luminosity ratio of the galaxies.

Subject headings: ISM: abundances, galaxies: abundances, galaxies: dwarf, galaxies: evolution, intergalactic medium

1. INTRODUCTION

Mass exchange between a galaxy and the intergalactic medium(IGM) can influence both the chemical composition of the galactic gas and the morphology of the galaxy. Several mechanisms for gas loss by a galaxy can be distinguished (Shustov et al. 1997): galactic wind induced by numerous supernova explosions, ram pressure exerted by the IGM, the tidal influence of other galaxies of the group, evaporation of gas due to interactions with the hot IGM, and blowing of the gas out of the galaxy by stellar radiation. Possible ways for the loss of stellar mass include tidal interactions, the ejection of stars due to the statistical mechanism, and the decay of stellar associations. Let us consider some of these mechanisms in more detail.

There have been many studies of the effects of numerous supernova explosions, such as galactic fountains, super-bubbles, and winds, on disk galaxies (see Shustov et al. (1997); Cooper et al. (2008) and references therein). The efficiency of these processes for gas ejection depends strongly on

the distribution of the gas. Thus, models of galaxies with a stratified interstellar medium (ISM) display a much higher mass-loss efficiency than do models with a continuous distribution of their ISM (Cooper et al. 2008). Computations of models with a continuous gas distribution, in turn, provide different results depending on the distribution law (Mac Low et al. 1989). It was shown in the theoretical study of De Young and Gallagher (1990) that the fraction of expelled gas in a $1.4 \times 10^9 M_\odot$ galaxy is ~ 0.6 , but, as the authors note, the presence of dark matter was not taken into account. According to Igumenshchev et al. (1990), galaxies with masses exceeding $10^{12} M_\odot$ do not have winds, and, hence, do not lose gas via this mechanism. Based on these computations, Shustov et al. (1997) used a simple approximation for the relation between the mass of the galaxy and the fraction of expelled matter in their models:

$$f_{\text{esc}} = 2.4 - 0.2 \lg \frac{M_G}{M_\odot} . \quad (1)$$

In this approximation, the efficiency of gas ejection becomes unity for galaxies with masses of $10^7 M_\odot$, irrespective of their morphology. According to this model, galaxies with such masses should not contain gas. At the same time, gas is almost completely absent only in spheroidal and elliptical dwarf galaxies, whereas it can constitute a substantial fraction of the masses of disk and irregular galaxies (Begum and Chengalur 2004; Karachentsev et al. 2004; Begum et al. 2008). On the other hand, observations have not revealed gas outflows into the IGM from galaxies with dynamical masses of $\sim 10^9 M_\odot$ (van Eymeren et al. 2009). Thus, the question of the efficiency of gas ejection due to galactic winds remains open.

Tidal interaction may be responsible not only for mass exchange between galaxies during collisions or close fly-bys and between galaxies and the IGM, but also for changes in galactic morphology. According to the estimates of Tutukov (2006), every galaxy in a cluster experiences a collision at least once during its lifetime. In these collisions, the galaxies may merge, lose their gaseous components, or be disrupted completely. A new galaxy may also form from gas lost in galaxy collisions.

The ram pressure of the IGM gas, evaporation of gas, and sweeping-out of dust are less efficient galactic mass-loss mechanisms, though they influence the chemical evolution of galaxies and enrichment of the IGM.

The essence of the statistical mechanism is that, in the case of an equilibrium distribution of the stars in the gravitational potential of the galaxy, there will always be stars with velocities exceeding the escape velocity. As these stars leave the potential well, the system relaxes to a new equilibrium state. However, the timescale for the statistical mechanism is very large — close to a hundred relaxation times (Binney and Tremaine 1987), where the latter is

$$\tau_{\text{relax}} \sim \frac{0.1N}{\ln N} \tau_{\text{dyn}} , \quad (2)$$

where N is the number of stars in the system and τ_{dyn} the dynamical timescale of the system. Typical galactic dynamical timescales are $\sim 10^7 - 10^8$ yr. Even for $\sim 10^6 M_\odot$ galaxies, the relaxation time exceeds the Hubble time. Other mass-loss mechanisms reviewed by Binney and Tremaine (1987) for collisionless stellar systems are even less efficient.

It is commonly believed that most stars are born in associations (see however, the paper by Elmegreen and Efremov (1996)). The lifetimes of OB associations from birth to decay is short, of the order of several million years. Typical velocities of stars acquired during the decay are of the order of 10 km/s, according to various studies (Gvaramadze and Bomans 2008) and observations (Gies 1987). Other estimates limit the velocity range to 2 – 8 km/s (Brown et al. 1997). The virial velocities in low-mass galaxies can be several km/s (Karachentsev et al. 2004), and the escape velocity lower than 20 km/s (Bovill and Ricotti 2009; Dijkstra et al. 2004). In the case of disk galaxies, the ordered motions of the galactic matter may facilitate the ejection of stars. The aim of our current study is to estimate this effect and observational manifestations in dwarf galaxies.

In Section 1, we compute the probability of ejection of stars from spheroidal and disk galaxies. In Section 2, we present the results of modeling the evolution of dwarf disk galaxies taking into account the ejection of stars. Section 3 discusses our results.

2. STELLAR EJECTION MECHANISM

To escape its galaxy, the kinetic energy of a star must be sufficient to bring about the work against the gravitational field

$$\frac{(\mathbf{v} + \mathbf{u})^2}{2} \geq -\Phi, \quad (3)$$

where \mathbf{v} is the instantaneous velocity of the OB association, \mathbf{u} the stellar velocity relative to the association, and Φ the gravitational potential at the location of the association, with the potential at infinity being zero. The dynamical timescales for associations ($\sim 10^8$ yr) exceed their lifetimes ($\sim 10^7$ yr) due to the low densities of associations, which are $0.1 M_{\odot}/\text{pc}^3$ (Brown et al. 1997). This means that energy equipartition for stars of different masses does not have time to become established in the association. Therefore, we will assume that the velocities of stars of any mass have isotropic Gaussian distributions with dispersion σ_{OB}^2 ; the probability that a star moving away from the center of the OB association will overcome the potential of its galaxy will then be

$$\chi(\mathbf{v}, -\Phi) = \int_{\frac{(\mathbf{v} + \mathbf{u})^2}{2} \geq -\Phi} \frac{d^3u}{(2\pi\sigma_{\text{OB}}^2)^{3/2}} \exp\left[-\frac{u^2}{2\sigma_{\text{OB}}^2}\right]. \quad (4)$$

The large-scale motion of the ISM in the galaxy increases the fraction of ejected stars due to a sort of “slingshot effect”. If the ISM participates in the Keplerian motion of the galaxy with circular velocity v , the velocity of a star after decay will be summed with the velocity of the association in the galaxy. As a result, the probability of ejection of the star becomes (see the Appendix)

$$\chi(\eta, \psi) = 1 + \frac{1}{4} \int_0^{\psi} d\xi e^{-\xi/2} \left\{ \operatorname{erf}\left[\frac{-\eta - \sqrt{\psi - \xi}}{\sqrt{2}}\right] - \operatorname{erf}\left[\frac{-\eta + \sqrt{\psi - \xi}}{\sqrt{2}}\right] \right\}, \quad (5)$$

where

$$\eta = \frac{v}{\sigma_{\text{OB}}} = \sqrt{\frac{r}{\sigma_{\text{OB}}^2} \frac{\partial \Phi}{\partial r}}, \quad \psi = -\frac{2\Phi}{\sigma_{\text{OB}}^2}. \quad (6)$$

Here, the velocity of the association is assumed to be equal to the local velocity of the ISM. The reason for this is that the lifetimes of associations are much shorter than the galactic dynamical timescale so the velocity of the association does not change appreciably before the association decays. The parameter η in Eq. 5 describes the relative velocity of the Keplerian motion in units of σ_{OB} . Expression 5 is also valid for galaxies in which large-scale motions of gas are absent, such as spheroidal galaxies, but we must then adopt $\eta = 0$.

The value of χ depends on the mass distribution in the galaxy and the motion of the galactic gas. It is interesting to estimate the fraction of ejected stars for some typical configurations of galaxies. We will calculate this estimate as an average over the volume of the galaxy weighted by their local star-formation rate Ψ :

$$\bar{\chi} = \frac{\int_V dV \Psi \chi}{\int_V dV \Psi}. \quad (7)$$

Let us give estimates for a spheroidal galaxy with a Plummer density profile and a disk galaxy with an exponential density profile.

The distributions of the density and potential in an isotropic Plummer sphere depend on two parameters — the mass M and the characteristic scale a :

$$\rho = \frac{3M}{4\pi a^3} (1 + r^2/a^2)^{-5/2}, \quad \Phi = -\frac{GM}{a} (1 + r^2/a^2)^{-1/2}. \quad (8)$$

Let us take the model of Firmani and Tutukov (1992) for the volume star-formation rate:

$$\Psi \propto \rho^2. \quad (9)$$

The distribution of the dimensionless potential ψ over the scale r/a depends only on the parameter β , which is defined as the ratio of the typical virial velocity in the galaxy and the velocity dispersion in the decaying association:

$$\psi = \frac{2\beta^2}{(1 + r^2/a^2)^{1/2}}, \quad \beta = \sqrt{\frac{GM}{\sigma_{\text{OB}}^2 a}}. \quad (10)$$

As we noted above, we assume $\eta \equiv 0$ for a spheroidal galaxy. Inserting these relations into Eq. 7 and integrating over the volume, we obtain the coefficient $\bar{\chi}$ as a function of β (Fig. 1, left panel, solid curve).

The distribution of the surface density of an exponential disk also depends on the total mass and spatial scale:

$$\Sigma = \frac{M}{2\pi a^2} e^{-r/a}. \quad (11)$$

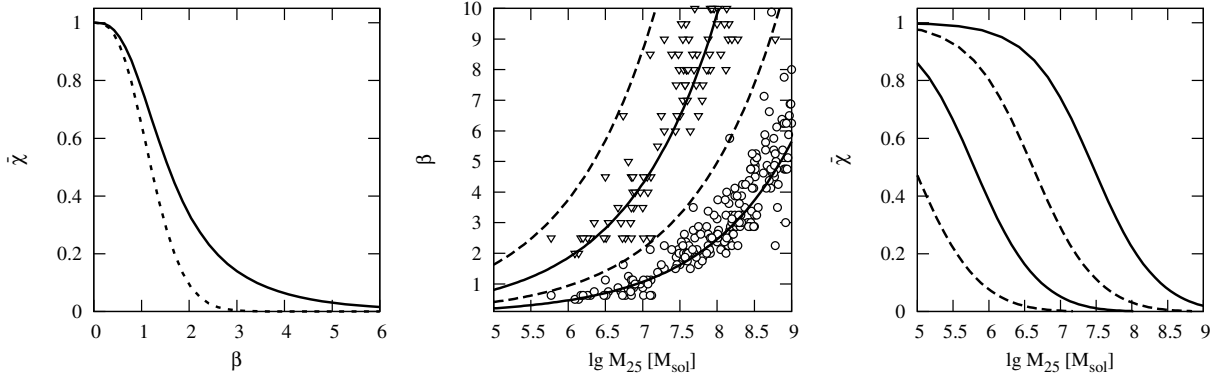


Fig. 1.— Left panel: average probability of ejection of stars from galaxies as a function of β , for disk galaxies with an exponential density profile and circular Keplerian rotation (solid) and non-rotating spheroidal galaxies with a Plummer density profile (dashed). The central panel shows β as a function of the mass of the galaxy (up to $10^9 M_\odot$). The mass distribution for the galaxies was taken from the catalog of nearby galaxies of Karachentsev et al. (2004). M_{25} is the dynamical mass within the 25^m isophote. The parameter β was computed as the ratio of the rotational velocity of neutral hydrogen (denoted in the catalog V_m) and the velocity dispersion in the decaying OB association σ_{OB} . Two limiting cases were considered for the latter: $\sigma_{OB} = 2$ km/s (triangles) and $\sigma_{OB} = 8$ km/s (circles). The solid lines show approximations for $\beta(M_{25})$ for these limiting cases. The dashed lines show analogous approximations for the ejection of stars outside the dark-matter halo (see the text). Right panel: dependence of the average probability of ejection of stars on the galaxy mass M_{25} . The lines correspond to the same cases as in central panel.

Let us apply an approximate expression for the gravitational potential, with the mass distribution taken to be spherically symmetric:

$$\Phi = -\frac{GM}{a} \frac{1 - e^{-r/a}}{r/a}. \quad (12)$$

In this approximation, as in the case of a Plummer sphere, the distributions for η and ψ depend only on β , which has the same definition:

$$\eta = \beta \sqrt{\frac{1 - (1 + r/a) e^{-r/a}}{r/a}}, \quad \psi = 2\beta^2 \frac{1 - e^{-r/a}}{r/a}. \quad (13)$$

Finally, let us take the surface density of the starformation rate according to the Schmidt–Kennicutt model (Kennicutt 1998):

$$\Psi \propto \Sigma^{3/2}. \quad (14)$$

The function $\bar{\chi}(\beta)$ for the two cases is plotted in Fig. 1 (left). For disk galaxies, the values of β for which the ejection of stars is possible are bounded from above by 4 – 5, while this limit is 2 – 2.5 for spheroidal galaxies. We used data from the Karachentsev catalog of nearby galaxies (Karachentsev et al. 2004) for galaxies with masses below $10^9 M_\odot$ to derive the dependence of β on the galactic mass. For each galaxy with a given mass, the value of β was calculated as the ratio of

the rotational velocity of neutral hydrogen (denoted in the catalog V_m) and the velocity dispersion of stars in the decaying OB association σ_{OB} . Since σ_{OB} can be in the range 2 – 8 km/s, the parameter β is also not determined precisely. The approximate mass dependence of this parameter is

$$\beta = 0.025 \left(\frac{M_{25}}{M_{\odot}} \right)^{0.36} \left(\frac{\sigma_{\text{OB}}}{\text{km/s}} \right)^{-1}. \quad (15)$$

In this approximation, we use the dynamical masses of the galaxies inside the 25 mag arcsec⁻² isophote, denoted M_{25} . Using only M_{25} for the mass underestimates the contribution of dark matter in the outer regions of the galaxy but the approximation 15 remains valid even if we take into account the dark haloes, viz. if we increase M_{25} by factor equals to $1 + \Omega_{\text{dm}}/\Omega_{\text{b}} \approx 6$, then the coefficient on the right-hand side becomes 0.048. The function 15 for the limiting values of σ_{OB} is shown in Fig. 1 (middle panel) for the cases when the dark-matter halo is and is not taken into account.

Below, we present results of our numerical modeling of dwarf galaxies in a single-zone approximation, taking into account the ejection of stars. We traced the chemical evolution of the galactic gas using the abundances of iron, oxygen and heavy elements. We used the model of Firmani and Tutukov (1992) and the studies of Shustov et al. (1997); Wiebe et al. (1998) as the basis for the one-zone model.

3. NUMERICAL MODELING

3.1. Single-zone Galactic Model

In a decaying association, only stars with lifetimes $\lesssim 10^7$ yr end their lives in the galaxy as Type II supernovae (SN II). These stars have masses of about $13 M_{\odot}$ and higher (Tutukov and Krugel 1980). Some fraction of lower-mass stars, whose number is determined by $\bar{\chi}$, leaves the galaxy and is not able to participate in the enrichment of the ISM. However, this effect may be small, since stars with masses below $8 M_{\odot}$ do not explode as SN II (Hashimoto et al. 1993), so that their disappearance influences the chemical composition of the ISM only more weakly. On the other hand, Type Ia supernovae (SN Ia) have delay times until their explosions of $10^8 - 10^9$ yr (Tutukov and Yungelson 2002), and their ejecta can strongly influence the enrichment of the ISM in metals. The mass fraction of all stars born as a single stellar population with a given initial mass function (IMF) $\Phi(m)$ and leaving the galaxy is $\bar{\chi} \int_{m_{\text{min}}}^{13M_{\odot}} dm \Phi$; for Salpeter IMF with index -2.35 and stellar mass range $0.1 M_{\odot} - 100 M_{\odot}$ this fraction is $0.88\bar{\chi}$.

In the single-zone approximation, the total rate of stellar mass loss due to the ejection of stars for a galaxy with a time-dependent star formation rate $\Psi(t)$ will be

$$\dot{M}_{\text{s}}^{\text{ej}}(t) = \bar{\chi} \Psi(t - \tau_{\text{s}}(13M_{\odot})) \int_{m_{\text{min}}}^{13M_{\odot}} dm \Phi, \quad (16)$$

where $\tau_s = \tau_s(m)$ is the lifetime of a star with mass m .

The ejection of stars also affects the amount of mass participating in star formation and chemical enrichment of the ISM. The rate of gas return is

$$\dot{M}_g^{\text{fb}}(t) = \int_{m_{\text{min}}}^{m_{\text{max}}} dm \Phi \Psi(t - \tau_s) \left(1 - \frac{m_r}{m}\right) [1 - \bar{\chi} \theta(13M_\odot - m)], \quad (17)$$

where $m_r = m_r(m)$ is the mass of the stellar remnant, $\theta(x) = 0$ for $x \leq 0$, and $\theta(x) = 1$ for $x > 0$. The rate of enrichment of the ISM in an element X is determined by the contributions from SN I and SN II:

$$\begin{aligned} \dot{M}_X^{\text{fb}}(t) = & \frac{10^{-3}}{M_\odot} \Psi(t - \tau_{\text{SN Ia}}) P_X^{\text{SN Ia}} [1 - \bar{\chi}] + \\ & + \int_{m_{\text{min}}}^{m_{\text{max}}} dm \Phi \Psi(t - \tau_s) \left[\left(1 - \frac{m_r}{m}\right) X(t - \tau_s) + P_X^{\text{SN II}}(m, Z(t - \tau_s)) \right] \times \\ & \times [1 - \bar{\chi} \theta(13M_\odot - m)], \quad (18) \end{aligned}$$

where $\tau_{\text{SN Ia}}$ is the average delay time between the formation of a binary and the SN Ia explosion, $P_X^{\text{SN Ia}}$ is the mass of element X ejected per explosion, and $P_X^{\text{SN II}}(m, Z)$ is the mass of element X produced by SN II with pre-supernova mass m and initial heavyelement abundance Z .

In this model, we assumed that SN Ia are produced by mergers of degenerate dwarfs in close binaries. As was shown by Tutukov and Yungelson (1994), the mean delay time between the formation of a binary and the SN Ia explosion is $\tau_{\text{SN Ia}} \approx 10^9$ yr. The rate of SN Ia explosions per unit star-formation rate is obtained by normalizing to the modern SN Ia rate of 0.003 per yr and modern star formation rate of $3 M_\odot$ per yr (Tutukov and Yungelson 1994). We assumed that each SN Ia produces $P_{\text{Fe}}^{\text{SN Ia}} = 0.6 M_\odot$ of iron (Tsujimoto et al. 1995); we did not consider the production of other elements by these supernovae. The yields of SN II as functions of the mass of the star and the initial heavy-element abundance were taken from Maeder (1992).

The balance of the total mass of galaxy, the mass of gas, and the masses of various elements is determined not only by star formation, but also by interaction of the galaxy with the ISM; i.e., via the galactic wind, dust ejection, and the accretion of intergalactic gas. These factors were studied previously for the same single-zone model (see, for instance, the study of Shustov et al. (1997)). However, accretion, dust ejection, and galactic wind were not taken into account in the present study [the last factor due to obvious shortcomings of the simple model for the galactic wind, Eq. 1]. As a result, the mass balances of various components of a galaxy was given by the equations:

$$\begin{aligned} \dot{M}_{\text{tot}} &= -\dot{M}_s^{\text{ej}} \\ \dot{M}_g &= -\Psi + \dot{M}_g^{\text{fb}} \\ \dot{M}_X &= -X\Psi + \dot{M}_X^{\text{fb}}. \end{aligned} \quad (19)$$

The details of this numerical model are presented in Firmani and Tutukov (1992); Shustov et al. (1997); Wiebe et al. (1998).

3.2. Results of the Computations

We can see from the dependence $\bar{\chi}(M_{25})$ (Fig. 1) that the decay of OB associations essentially does not lead to mass loss from spheroidal galaxies, even those with the lowest masses. For this reason, we restricted our numerical analysis to disk galaxies. We computed four series of models for the evolution of galaxies with masses from $10^{6.5} M_{\odot}$ to $10^{8.5} M_{\odot}$ and various values of σ_{OB} . For comparison, we also computed a series of closed models. The radii of the galaxies corresponded to the relation $M \propto R^2$. To avoid a large influence of the initial conditions on the burst of star formation, the semi-thickness of the protogalactic disk was set to 10 kpc in all computations. The remaining parameters for the computed series of models are given in the table. In series A, $\sigma_{\text{OB}} = 2$ km/s, while in series B and C $\sigma_{\text{OB}} = 8$ km/s. In series C, we allowed for the influence of the dark-matter halo [see the comments concerning Eq. 15]. Thus, the series B computations enabled us to estimate the effects of ejecting stars from the disk into the galactic halo, while series C illustrated the effects of ejecting stars from the halo into the IGM.

		$\sigma_{\text{OB}} = 2$ km/s (series A)		$\sigma_{\text{OB}} = 8$ km/s (series B)		$\sigma_{\text{OB}} = 8$ km/s +dark halo (series C)	
$\lg M/M_{\odot}$	R , pc	β	$\bar{\chi}$	β	$\bar{\chi}$	β	$\bar{\chi}$
6.5	79.5	2.73	0.21	0.70	0.92	1.38	0.6
7	141.4	4.14	0.09	1.07	0.743	2.08	0.32
7.5	251.5	6.26	0.012	1.62	0.481	3.16	0.13
8	447	9.48	~ 0	2.45	0.21	4.78	0.035
8.5	795	14.25	~ 0	3.72	0.075	7.23	~ 0

Figure 2 shows the integrated characteristics of the model galaxies at the end of the computations. As expected, including the ejection of stars in the series A models did not result in significant deviations of the integrated characteristics from those for the closed model. In the series B and C models, for the lowest mass galaxies, the ratio of the ejected mass and the dynamical mass can range from 1.5 – 2 (for matter ejected from the halo into the IGM) to 6 (for matter ejected from the disk into the halo). The amount of ejected mass obtained in the series B models provides some idea of the extent to which the morphology of a galactic disk can vary. For a galaxy with dynamical mass $10^7 M_{\odot}$, the stellar mass in the halo exceeds the mass of the disk by a factor of 1.5 – 2; i.e., such a galaxy cannot be considered a disk galaxy. Galaxies with final dynamical masses of $10^6 M_{\odot}$ can have a mass of $4.5 \times 10^6 M_{\odot}$ in the halo and $1.5 \times 10^6 M_{\odot}$ in the IGM. The mass–luminosity relation shows that, compared to the closed model, the total luminosity of the lowest-mass galaxies can be half an order of magnitude lower, and the disk luminosity an order of magnitude lower. The mass-to-luminosity ratio itself increases by more than a factor of 2.5 for the low-mass galaxies of series B. For series B galaxies with masses below $10^7 M_{\odot}$, the total luminosity of stars ejected into the halo is a factor of two to three higher than the disk luminosity (Fig. 2, middle panel in the

upper row). This also provides evidence for the transformation of the galactic morphology from disk to spheroidal.

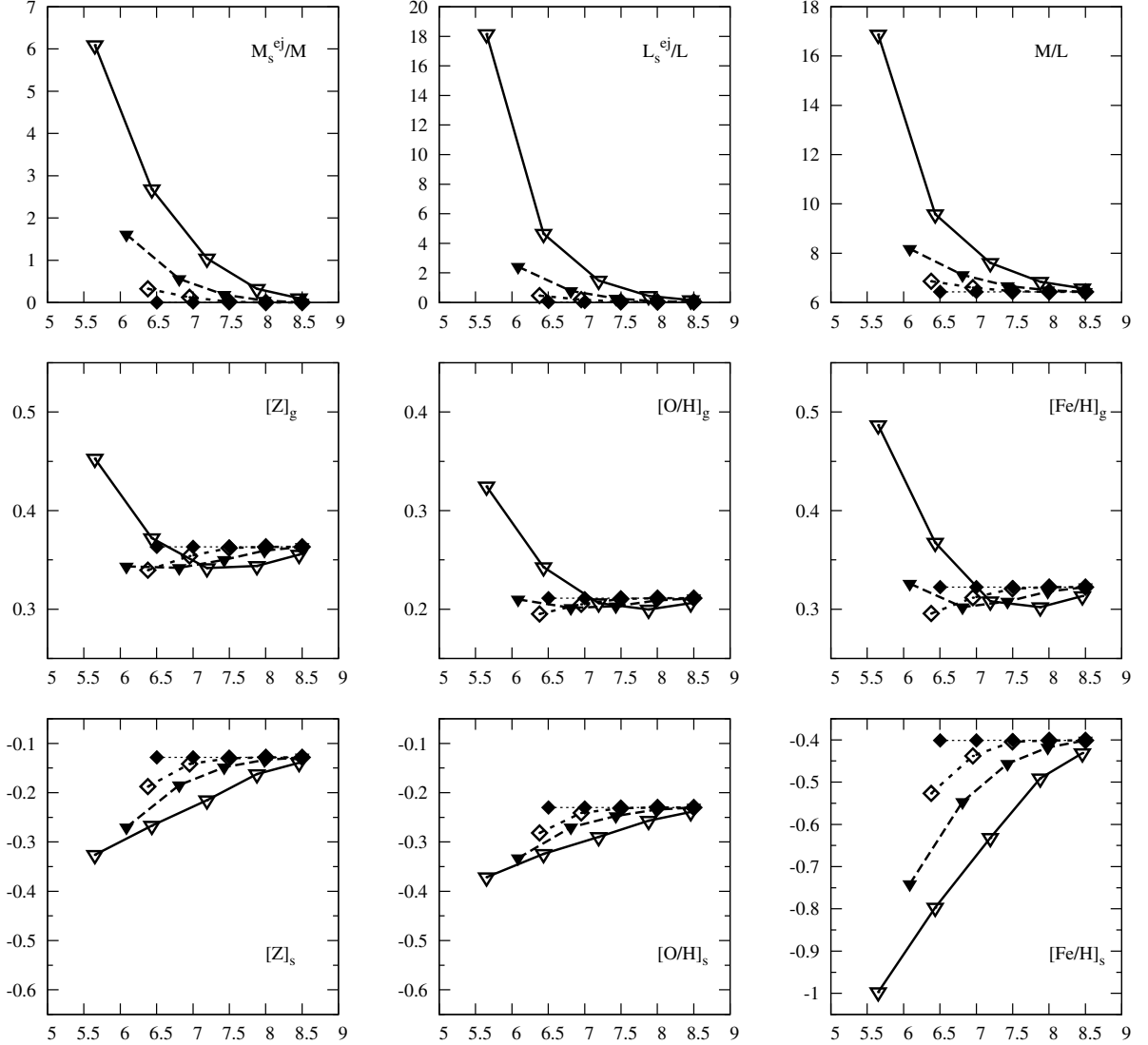


Fig. 2.— Dependence of integrated parameters on the disk masses (on a logarithmic scale in units of M_\odot) in four series of models. Solid diamonds correspond to the closed galaxy model, open diamonds to the model with $\sigma_{OB} = 2$ km/s (series A), solid triangles to the model with $\sigma_{OB} = 8$ km/s plus a dark-matter halo (series C), and open triangles to the model with $\sigma_{OB} = 8$ km/s without a dark-matter halo (series B). The upper row of plots shows the ratio of the ejected mass and disk mass, the ratio of the luminosities of the ejected stars and the disk, and the mass-to-luminosity ratio for the disk (in solar units). The panels in the middle and lower rows show the abundances of various elements in the gas and stars (averaged over the stellar population).

Since we did not consider galactic wind and accretion in our models, the star-formation history in the galaxies consisted of a single burst which depleted most of the gas: in all the galaxies, the

mass fraction of the gas at the end of the computations was 5 – 10%. The relative abundances of elements in the gas decrease weakly with the mass of the galaxy and with increasing σ_{OB} (Fig. 2, middle row of plots). One exception is the models at the low-mass end of series B, for which the relative abundances of element grow with the galaxy mass by 0.1 dex, compared to the closed models. As the plots show, in all series of models, the mass dependence of the abundances converges to a minimum for some mass in all series of models. The reason for this may be a competition of two processes determining the abundances in the gas: the enrichment of gas by supernovae and the return of gas poor in elements by explosions of new low-mass stars. The influence of the latter process may be diminished if a galaxy loses a considerable fraction of its low-mass stars.

The elemental abundances in the stars systematically decrease with the mass of the galaxy and with increasing σ_{OB} (Fig. 2, lower row of plots). The ejection of stars influences the iron abundance most. In a galaxy with dynamical mass $10^6 M_{\odot}$, the iron abundance can decrease by 0.5 dex in the disk stars (series B) and by more than 0.3 dex in the halo stars (series C). Figure 3 shows the distribution of the relative numbers of stars over the abundances of iron, oxygen, and heavy elements for all the computed series of models. Series B (second column of plots) differs most from the closed model. Along with the shift of the distribution toward lower abundances, stars heavily enriched in iron appear, which formed in the first few billion years after the SN Ia explosions. The characteristic appearance of the stellar distributions is due to the fact that the galaxies in this model experience only one burst of star formation, which occurred in a low-metallicity gas.

4. DISCUSSION AND CONCLUSIONS

We have studied the influence of the loss of stellar mass on the evolution of dwarf spheroidal and disk galaxies. The decay of OB associations was considered as a possible mass-loss mechanism, with the decay enabling some stars to obtain velocities sufficient to escape their galaxy. The decay of associations is essentially of no importance for the evolution of spheroidal galaxies. The effect is also small for disk galaxies with $\sigma_{\text{OB}} = 2$ km/s. Since a value of ~ 10 km/s is thought to be typical, we focused our analysis on models with $\sigma_{\text{OB}} = 8$ km/s. The results of our analysis are as follows.

1. During the lifetime of an OB association ($\sim 10^7$ yr), the most massive SN II ($\gtrsim 13 M_{\odot}$) are able to enrich the ISM in the products of their explosions. Lower-mass stars that leave their galaxy do not contribute to the enrichment of the disk ISM, but instead serve as a source of elements for the halo or IGM. The same is true of SNIa.
2. Disk galaxies that had at the onset of their star formation masses of $3 \times 10^7 M_{\odot}$ contain half of their mass in disk stars and the other half in the halo. The halo luminosities in such galaxies exceed the disk luminosities by a factor 1.52. We can thus infer that galaxies with masses $\lesssim 10^7 M_{\odot}$ that were initially disk galaxies change their morphology to spheroidal. According to the classification of de Vaucouleurs et al. (1991), spiral galaxies are assigned morphological indices $T = 4$ (see also Corwin et al. (1994)). In the catalog of nearby galaxies

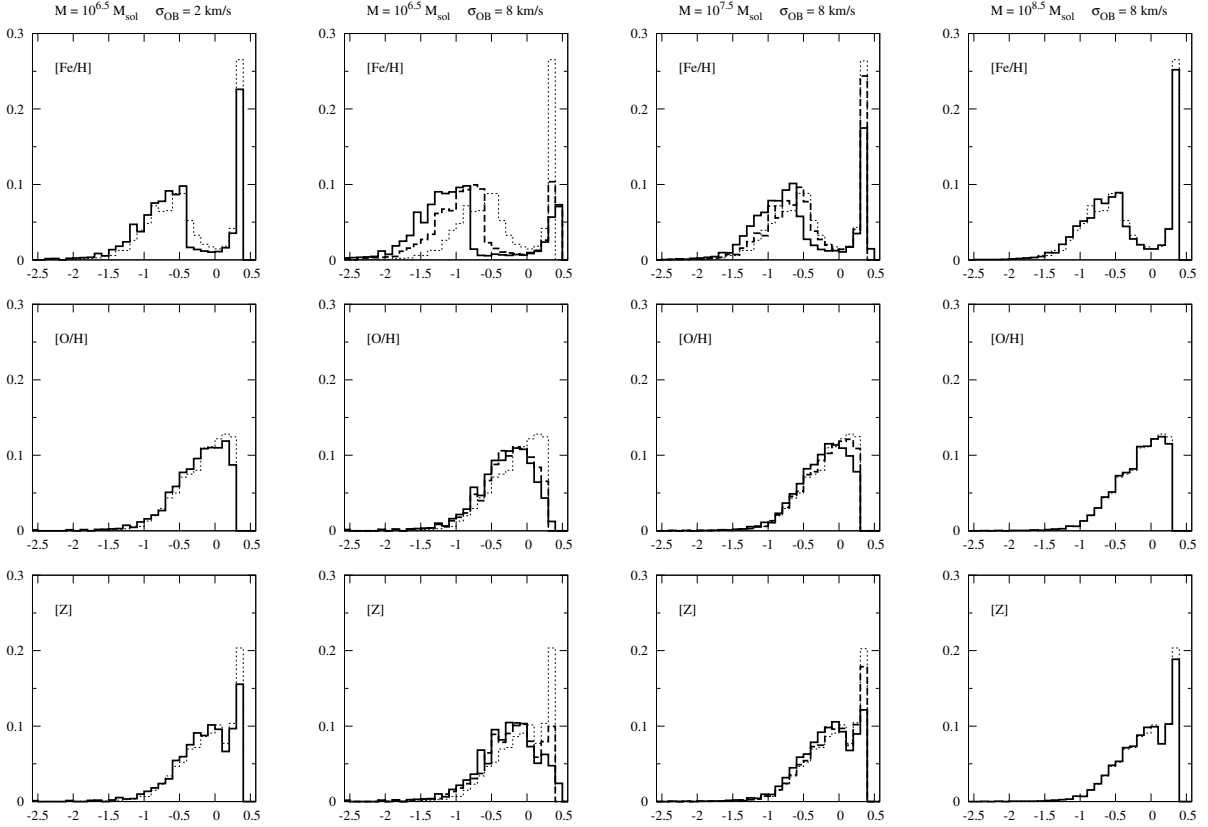


Fig. 3.— Distribution of the relative number of stars over the current abundances of iron, oxygen, and heavy elements. In the left column, the solid curves correspond to galaxies with masses of $10^{6.5} M_{\odot}$ in the series A models, and the thin dotted curve to the closed model. In the other columns, the solid curves correspond to galaxies with masses of $10^{6.5} M_{\odot}$, $10^{7.5} M_{\odot}$, and $10^{8.5} M_{\odot}$ in the series B models, the dashed curves to galaxies with the same masses in the series C models, and the thin dotted curves to the closed model.

(Karachentsev et al. 2004), disk galaxies have absolute magnitudes not exceeding -13^m (for morphological indices from 0 to 7; i.e., including lenticular and irregular galaxies that are closest to disk galaxies); this magnitude corresponds to a luminosity $\sim 10^7 L_{\odot}$ and a galactic mass $\sim 10^8 M_{\odot}$. Lower-mass galaxies are classified as spheroidal and irregular. This is confirmed by the computations for the models we have adopted here.

3. In systems with masses $\lesssim 10^5 M_{\odot}$, a large fraction of the stellar mass leaves not only the disk of the galaxy, but also the halo (Fig. 1, right panel). Thus, if extremely low-mass galaxies can form at all, they can lose almost all their stellar population to the IGM after their first burst of star formation. As a result, a dark-matter halo enriched in gas should be left. This scenario may be important for the problem of missing satellites of the Galaxy.
4. The ejection of stars increases the mass-to-luminosity ratio. For galaxies with total masses (disk + halo) of $\sim 10^7 M_{\odot}$, this ratio increases by a factor of 2 – 2.5 (Fig. 2, upper right

panel).

5. The ejection of stars may result in strong variations of elemental abundances in the gas (Fig. 2, middle row of plots): along with the systematic decrease of the abundances by ~ 0.05 dex, the elemental abundances in the lowest-mass galaxies can increase by $0.1 - 0.15$ dex. The abundances in stars systematically fall with the galaxy mass decrease, by 0.2 dex.

This study was supported by the Federal Agency on Science and Innovation (state contract no. 02.740.11.0247), the Federal Education Agency (contract RNP-2.1.1-1937), the Program of State Support for Leading Scientific Schools of the Russian Federation (grant no. NSh-4354.2008.2), and the Russian Foundation for Basic Research (project nos. 08-02-91321-IND and 07-02-00454).

APPENDIX

We will obtain an expression for the probability of ejection of a star from an OB association moving along a Keplerian orbit in a galaxy with a given gravitational potential $\Phi(r)$. A general expression for this probability is

$$\chi(\mathbf{v}, -\Phi) = \int_{\frac{(\mathbf{v}+\mathbf{u})^2}{2} \geq -\Phi} \frac{d^3u}{(2\pi\sigma_{\text{OB}})^{3/2}} \exp\left[-\frac{u^2}{2\sigma_{\text{OB}}^2}\right]. \quad (20)$$

The velocity vector for a circular Keplerian orbit is

$$\mathbf{v} = \mathbf{e}_\phi v, \quad v = \sqrt{r \frac{\partial\Phi}{\partial r}}, \quad (21)$$

where \mathbf{e}_ϕ is a unit vector in the azimuthal direction. The integration domain is in this case described by the equation

$$u_\phi^2 + u_\perp^2 + 2vu_\phi + v^2 + 2\Phi \geq 0, \quad (22)$$

where u_\perp is the modulus of the velocity orthogonal to \mathbf{e}_ϕ . Solving this equation leads to the condition for the velocity component u_ϕ

$$u_\phi \in (-\infty, \Re(u_{\phi-})] \cup [\Re(u_{\phi+}), +\infty), \quad u_{\phi\pm} = -v \pm \sqrt{-2\Phi - u_\perp^2}. \quad (23)$$

Since the components of the vector \mathbf{u} are distributed isotropically and are independent, we can integrate the general expression over u_ϕ . Introducing the notation

$$\xi = \frac{u_\perp^2}{\sigma_{\text{OB}}^2}, \quad \eta = \frac{v}{\sigma_{\text{OB}}}, \quad \psi = -\frac{2\Phi}{\sigma_{\text{OB}}^2}, \quad (24)$$

we finally obtain

$$\chi(\eta, \psi) = 1 + \frac{1}{4} \int_0^\psi d\xi e^{-\xi/2} \left\{ \operatorname{erf}\left[\frac{-\eta - \sqrt{\psi - \xi}}{\sqrt{2}}\right] - \operatorname{erf}\left[\frac{-\eta + \sqrt{\psi - \xi}}{\sqrt{2}}\right] \right\}. \quad (25)$$

If $\eta \equiv 0$, the general expression 20 reduces to

$$\chi(\psi) = \sqrt{\frac{2}{\pi}} \int_{\psi}^{\infty} d\zeta \zeta^2 e^{-\zeta^2/2} = 1 - \operatorname{erf} \left[\sqrt{\frac{\psi}{2}} \right] + \sqrt{\frac{2}{\pi}} \sqrt{\psi} e^{-\psi/2}. \quad (26)$$

REFERENCES

- A. Begum and J. N. Chengalur. Kinematics of the faintest gas-rich galaxy in the Local Group: DDO210. *A&A*, 413:525–534, January 2004. doi: 10.1051/0004-6361:20031549.
- A. Begum, J. N. Chengalur, R. C. Kennicutt, I. D. Karachentsev, and J. C. Lee. Life in the last lane: star formation and chemical evolution in an extremely gas rich dwarf. *MNRAS*, 383: 809–816, January 2008. doi: 10.1111/j.1365-2966.2007.12592.x.
- J. Binney and S. Tremaine. *Galactic dynamics*. 1987.
- M. S. Bovill and M. Ricotti. Pre-Reionization Fossils, Ultra-Faint Dwarfs, and the Missing Galactic Satellite Problem. *ApJ*, 693:1859–1870, March 2009. doi: 10.1088/0004-637X/693/2/1859.
- A. G. A. Brown, G. Dekker, and P. T. de Zeeuw. Kinematic ages of OB associations. *MNRAS*, 285: 479–492, March 1997.
- J. L. Cooper, G. V. Bicknell, R. S. Sutherland, and J. Bland-Hawthorn. Three-Dimensional Simulations of a Starburst-driven Galactic Wind. *ApJ*, 674:157–171, February 2008. doi: 10.1086/524918.
- H. G. Corwin, Jr., R. J. Buta, and G. de Vaucouleurs. Corrections and additions to the third reference catalogue of bright galaxies. *AJ*, 108:2128–2144, December 1994. doi: 10.1086/117225.
- G. de Vaucouleurs, A. de Vaucouleurs, H. G. Corwin, Jr., R. J. Buta, G. Paturel, and P. Fouque. *Third Reference Catalogue of Bright Galaxies*. 1991.
- D. S. De Young and J. S. Gallagher, III. Selective loss of metals from low-mass galaxies. *ApJ*, 356: L15–L19, June 1990. doi: 10.1086/185740.
- M. Dijkstra, Z. Haiman, M. J. Rees, and D. H. Weinberg. Photoionization Feedback in Low-Mass Galaxies at High Redshift. *ApJ*, 601:666–675, February 2004. doi: 10.1086/380603.
- B. G. Elmegreen and Y. N. Efremov. An Extension of Hierarchical Star Formation to Galactic Scales. *ApJ*, 466:802–+, August 1996. doi: 10.1086/177554.
- C. Firmani and A. Tutukov. Evolutionary models for disk galaxies. *A&A*, 264:37–48, October 1992.
- D. R. Gies. The kinematical and binary properties of association and field O stars. *ApJS*, 64: 545–563, July 1987. doi: 10.1086/191208.

- V. V. Gvaramadze and D. J. Bomans. Search for OB stars running away from young star clusters. I. NGC 6611. *A&A*, 490:1071–1077, November 2008. doi: 10.1051/0004-6361:200810411.
- M. Hashimoto, K. Iwamoto, and K. Nomoto. Type II supernovae from 8-10 solar mass asymptotic giant branch stars. *ApJ*, 414:L105–L108, September 1993. doi: 10.1086/187007.
- I. V. Igumenshchev, B. M. Shustov, and A. V. Tutukov. Dynamics of supershells - Blow-out. *A&A*, 234:396–402, August 1990.
- I. D. Karachentsev, V. E. Karachentseva, W. K. Huchtmeier, and D. I. Makarov. A Catalog of Neighboring Galaxies. *AJ*, 127:2031–2068, April 2004. doi: 10.1086/382905.
- R. C. Kennicutt, Jr. The Global Schmidt Law in Star-forming Galaxies. *ApJ*, 498:541–+, May 1998. doi: 10.1086/305588.
- M.-M. Mac Low, R. McCray, and M. L. Norman. Superbubble blowout dynamics. *ApJ*, 337:141–154, February 1989. doi: 10.1086/167094.
- A. Maeder. Stellar yields as a function of initial metallicity and mass limit for black hole formation. *A&A*, 264:105–120, October 1992.
- B. Shustov, D. Wiebe, and A. Tutukov. Evolution of disk galaxies and loss of heavy elements into the intracluster medium. *A&A*, 317:397–404, January 1997.
- T. Tsujimoto, K. Nomoto, Y. Yoshii, M. Hashimoto, S. Yanagida, and F.-K. Thielemann. Relative frequencies of Type Ia and Type II supernovae in the chemical evolution of the Galaxy, LMC and SMC. *MNRAS*, 277:945–958, December 1995.
- A. V. Tutukov. The role of external factors in the evolution of galaxies. *Astronomy Reports*, 50: 439–450, June 2006. doi: 10.1134/S1063772906060035.
- A. V. Tutukov and E. Krugel. Stellar evolution and some parameters of galaxies and their nuclei. *AZh*, 57:942–952, October 1980.
- A. V. Tutukov and L. R. Yungelson. Merging of Binary White Dwarfs Neutron Stars and Black-Holes Under the Influence of Gravitational Wave Radiation. *MNRAS*, 268:871–+, June 1994.
- A. V. Tutukov and L. R. Yungelson. A Model for the Population of Binary Stars in the Galaxy. *Astronomy Reports*, 46:667–683, August 2002. doi: 10.1134/1.1502227.
- J. van Eymeren, M. Marcelin, B. Koribalski, R.-J. Dettmar, D. J. Bomans, J.-L. Gach, and P. Balard. A kinematic study of the irregular dwarf galaxy NGC 2366 using H i and H α observations. *A&A*, 493:511–524, January 2009. doi: 10.1051/0004-6361:200809585.
- D. S. Wiebe, A. V. Tutukov, and B. M. Shustov. On the evolution of the star formation rate in disk galaxies. *Astronomy Reports*, 42:1–10, January 1998.

